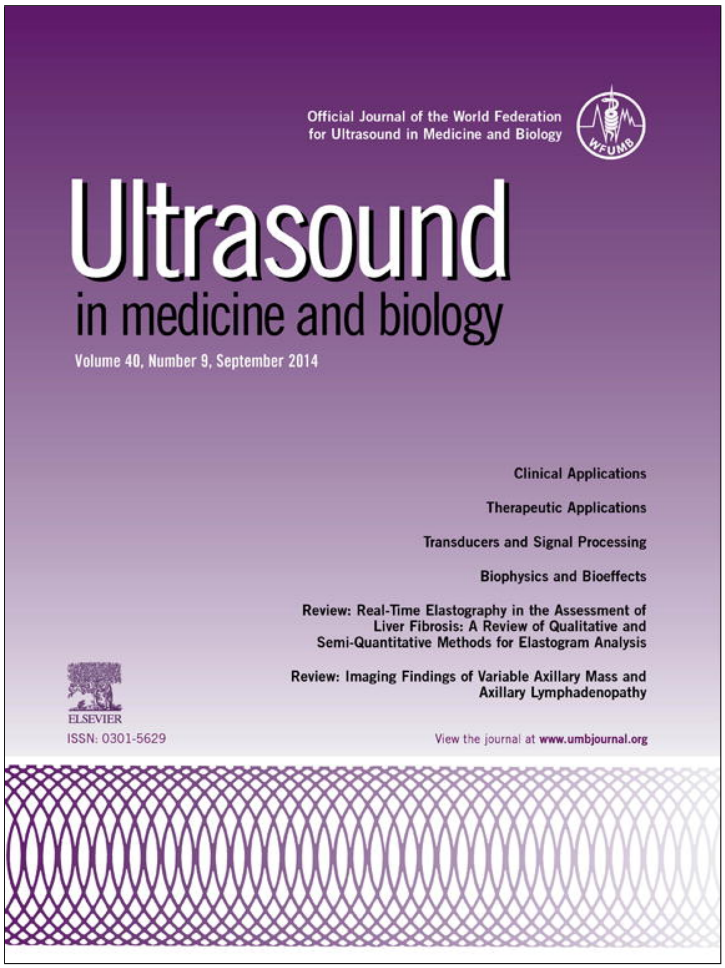
Official Journal of the World Federation
for Ultrasound in Medicine and Biology
WFUMB
Ultrasound
in medicine and biology
Volume 40, Number 9, September 2014
Clinical Applications
Therapeutic Applications
Transducers and Signal Processing
Biophysics and Bioeffects
Review: Real-Time Elastography in the Assessment of Liver Fibrosis: A Review of Qualitative and Semi-Quantitative Methods for Elastogram Analysis
Review: Imaging Findings of Variable Axillary Mass and Axillary Lymphadenopathy
ELSEVIER
ISSN: 0301-5629
View the journal at www.umbjournal.org

Ultrasound in Med. & Biol., Vol. 40, No. 9, pp. 2096–2106, 2014

0301-5629/$ - see front matter

http://dx.doi.org/10.1016/j.ultrasmedbio.2014.04.017

SHORT- AND LONG-TERM EFFECTS ON THE CILIARY BODY AND THE AQUEOUS OUTFLOW PATHWAYS OF HIGH-INTENSITY FOCUSED ULTRASOUND CYCLOCOAGULATION

Florent Aptel,*† Aurélie Béglé,‡ Arash Razavi,‡§¶ Fabrice Romano,‡ Thomas Charrel,‡ Jean-Yves Chapelon,§¶ Philippe Denis,‖ and Cyril Lafon§¶

*University Hospital of Grenoble, Grenoble, France; †Université Grenoble Alpes, Grenoble, France; ‡EyeTechCare, Rillieux la Pape, France; §Inserm, U1032, Lyon, F-69003, France; ¶Université de Lyon, Lyon, France; and ‖Hospices Civils de Lyon, Lyon, France

(*Received* 16 *December* 2013; *revised* 23 *April* 2014; *in final form* 26 *April* 2014)

Abstract—Several physical methods can be used to coagulate the ciliary body and decrease intra-ocular pressure in patients with glaucoma. The study described here investigated the short- and long-term effects of high-intensity focused ultrasound (HIFU) cyclocoagulation on the aqueous humor production structures and outflow pathways. Thirty-four rabbit eyes were sonicated with a ring-shaped probe containing six miniaturized HIFU transducers. Light, scanning electron and transmission electron microscopy and corrosion casts were performed. In the affected regions, the epithelium of the ciliary processes was degenerated or necrotic and sloughed off. Examinations performed several months afterward revealed involution of the ciliary processes. Vascular corrosion cast revealed focal interruption of the ciliary body microvasculature. In most animals, a sustained fluid space was seen between the sclera, the ciliary body and the choroid, likely indicating an increase in the aqueous outflow by the uveoscleral pathway. These results suggest that HIFU cyclocoagulation has a dual effect on aqueous humor dynamics. (E-mail: faptel@chu-grenoble.fr)

Key Words: **High-intensity focused ultrasound, Ciliary body, Aqueous outflow, Glaucoma, Histopathology, Scanning electron microscopy, Corrosion cast, Intravascular latex injection.**

INTRODUCTION

Many methods and energy sources for destroying ciliary processes that result in coagulation necrosis of the ciliary body after heating (laser, microwave) or freezing (cryotherapy) have been investigated (Al-Ghamdi et al. 1993; De Roetth 1965; Hamard et al. 1997; Kosoko et al. 1996; Maus and Katz 1990; Sabri and Vernon 1999; Uram 1992; Vernon et al. 2006). All these methods have two major drawbacks that limit their clinical use. First, they are non-selective of the organ to be treated, often resulting in damage to adjacent structures and ocular inflammation. Laser energy is absorbed mainly by pigmented tissues and, therefore, can also damage the iris and the choroid. Cryotherapy and cyclodiathermy also result in a large area of treatment with unpredictable dimensions. Second, these methods have an unpredictable dose–effect relationship, which prevents accurate prediction of the treatment effect. Published studies report a 6% to 64.3% risk of visual acuity decrease, 0.5% to 37.5% risk of ocular phthisis, 12.4% to 27% risk of chronic inflammation, 2% to 6% risk of corneal dystrophy, 10% to 35% risk of cataract formation and 12.9% to 80% risk of failure 1 y after the procedure (Al-Ghamdi et al. 1993; De Roetth 1965; Hamard et al. 1997; Kosoko et al. 1996; Maus and Katz 1990; Sabri and Vernon 1999; Uram 1992; Vernon et al. 2006).

To overcome the drawbacks of current and past methods of cyclodestruction, and taking advantage of recent breakthroughs in the field of high-intensity focused ultrasound (HIFU) technology, a new device was recently developed with the aim of achieving selective and precise destruction of the ciliary body and sparing the adjacent ocular structures (Aptel and Lafon 2012; Aptel et al. 2010, 2011; Charrel et al. 2011). In the first animal study designed to evaluate the feasibility and safety of the method, we treated rabbits using this device and then performed histologic examinations of the anterior

Address correspondence to: Florent Aptel, Department of Ophthalmology, University Hospital of Grenoble, 38043 Grenoble Cedex 09, France. E-mail: faptel@chu-grenoble.fr

segment focused on the ciliary body and ciliary processes (Aptel et al. 2010). We observed selective and circumferentially distributed coagulation necrosis of the ciliary processes and ciliary body. The bilayered epithelium was degenerated or necrotic and sloughed off in the distal parts of the most affected areas. The sclera from all treated areas appeared normal with no signs of thinning or necrosis. We therefore hypothesized that the decrease in intra-ocular pressure (IOP) after ultrasound cyclocoagulation is due mainly to a reduction in aqueous humor production by the ciliary body. Clinical studies were then started in patients with refractory glaucoma (Aptel et al. 2011; Aptel and Lafon 2012), with ultrasound biomicroscopy examinations of the treated eyes before and after treatment. In the pilot human study, cystic involution of the ciliary body was observed in 9 of the 12 eyes, with multiple hypo-echoic ovoid cystic cavities. Hyporeflective suprachoroidal fluid space was observed in 8 of the 12 eyes. Patients with hypo-reflective suprachoroidal space had significantly lower IOP than those without visible suprachoroidal space. We supposed that this may indicate increased uveoscleral outflow through the supraciliary and suprachoroidal space.

Many mechanisms have been advanced to explain IOP reduction after cyclodestruction or cyclophotocoagulation in previously published studies, including destruction of the pigmented and non-pigmented epithelium resulting in reduced aqueous production, vascular depletion of the ciliary body, ciliary body inflammation, enhanced uveoscleral outflow caused by changes in the ciliary body stroma and damage to the pars plana (Aptel and Lafon 2012; Blasini et al. 1990; Ferry et al. 1995; Liu et al. 1994; Schubert and Federman 1989). The present study was therefore conceived to qualitatively investigate by histologic studies the possible short- and long-term effects of high-intensity focused ultrasound cyclocoagulation on the aqueous humor production structures and aqueous outflow pathways.

METHODS

High-intensity focused ultrasound device, procedures and follow-up

The HIFU device was previously described in detail (Aptel et al. 2010; Charrel et al. 2011). A coupling cone made of polymer was placed in direct contact with the eye, which allowed good placement of the transducers in terms of centering and distance. At the base of the coupling cone, a suction ring allowed the application of a low-level vacuum and enabled the cone to maintain contact with the eye. A 30-mm-diameter, 15-mm-high ring containing six active piezoelectric elements was inserted in the upper part of the coupling cone (Fig. 1). The cavity created between the eye, the cone and the probe (5 mL) was filled through the central aperture of the device with room temperature saline solution. Each of the six transducers was a segment of a 10.2-mm-radius cylinder with a 4.5-mm width and a 7-mm length. The focal volume of each transducer had approximately an elliptic cylinder shape. The six transducers were placed at regular intervals on the upper and inferior circumference of the ring, avoiding the nasal and temporal meridians, and were oriented to create a focal zone consisting of six regularly distributed elliptical cylinder-shaped volumes. The six elliptical cylinder-shaped volumes were centered on a 12-mm-diameter circle, adapted to the anatomy of the rabbit ciliary body. The transducers were operated at the frequency of 21 MHz. The ring was connected to a control module, which allowed each sector to be sequentially activated according to a program defined by the operator.

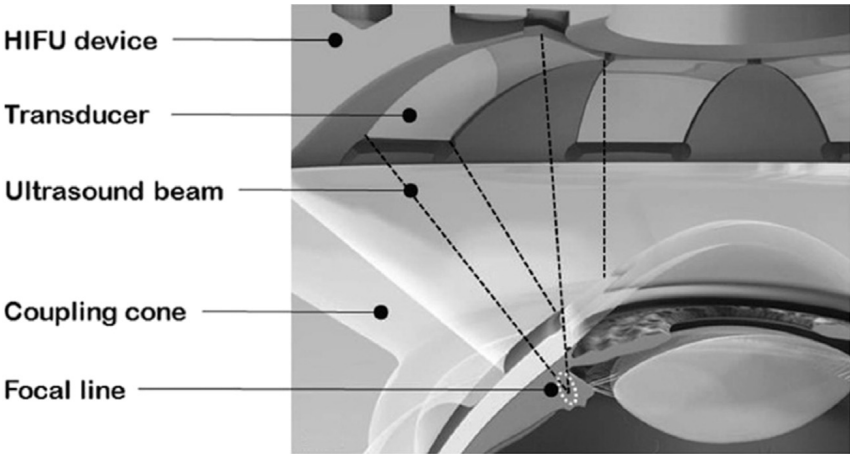

Fig. 1. Schematic cross section of the device and the coupling cone. HIFU = high-intensity focused ultrasound.

Table 1. IOP at baseline and during follow-up in treated and control eyes

	IOP of treated eyes	*p* (paired *t*-test, comparison to day 0 value)	IOP of control eyes	*p* (paired *t*-test, comparison to day 0 value)
Day 0 (before treatment)	10.4 ± 1.5 (n = 34)	NA	10.2 ± 1.6 (n = 8)	NA
Day 5	6.9 ± 1.4 (n = 34)	<0.0001	9.9 ± 1.3 (n = 8)	0.69
Day 10	7.2 ± 2 (n = 28)	<0.0001	10 ± 2.2 (n = 5)	0.82
Day 20	7.1 ± 1.7 (n = 28)	<0.0001	10.7 ± 1.1 (n = 5)	0.76
Day 30	7.6 ± 1.2 (22)	<0.0001	10.7 ± 0.8 (n = 5)	0.78
Day 60	6.9 ± 1 (n = 18)	<0.0001	9.7 ± 1.7 (n = 5)	0.54
Day 90	7.4 ± 1 (n = 14)	<0.0001	9.6 ± 0.9 (n = 5)	0.58
Day 120	7.5 ± 1.2 (n = 10)	<0.0001	9.8 ± 0.9 (n = 5)	0.64
Day 150	7.0 ± 1.1 (n = 10)	<0.0001	10.0 ± 1.1 (n = 5)	0.80
Day 180	7.3 ± 0.9 (n = 10)	<0.0001	10.2 ± 0.9 (n = 5)	0.85

IOP = intra-ocular pressure.

Twenty-one female adult New Zealand White rabbits (Charles River Laboratories, l'Arbresle, France) were treated. This study was approved by the Institut Claude Bourgelat institutional review board and ethics committee (Vetagro-Sup, Marcy l'Etoile, France), and was conducted in accordance with the requirements of EU Directive 2010/63/EU for animal experiments. The rabbits were anesthetized with ketamine hydrochloride (40 mg/kg intramuscular Ketamine 1000, Virbac, Carros, France) and xylazine (5 mg/kg, Bayer Santé, Loos, France). Drops of tetracaine (Faure, Annonay, France) were applied to the surface of the eye. The coupling cone was applied so that the truncated side was in contact with the peripheral cornea at the limbus. The active ring with the six piezoelectric elements was placed on the cone. Once the ring was placed on the cone, 5 mL of saline solution was used to fill the device until the fluid level reached the upper ring aperture, acting as coupling fluid and cooling the transducers. Before each treatment, the type of shot was configured on the control module. The parameters set were number of sectors to be activated, duration of shots and periods between shots and acoustic power. The following parameters were used: number of sectors activated, 6; acoustic power, 2.45 W; duration of each of the six shots, 8 s; time between each shot, 10 s. Thirty-four eyes from 21 rabbits were treated; 8 eyes from 21 rabbits were used as controls (for each of these 8 rabbits, one eye was treated and one eye was used as the control).

Intra-ocular pressure was measured bilaterally on day 0 before treatment and after treatment at days 5, 10, 20, 30, 60, 90, 120, 150 and 180 using a portable tonometer (Tono-pen XL, Reichert, Depew, NY, USA). The rabbits were anesthetized for IOP measurements with the same procedures described above. The measurements were taken at least 5 min after the induction of general anesthesia and under the same conditions at all time points. Ten series of measurements were taken by one operator. If the standard deviation for one series (indicated by the tonometer) was >5%, the measurements were repeated until a standard deviation ≤5% was obtained for each series. On day 5, the lids and the anterior segment were examined with a portable slit-lamp biomicroscope (Model SL-15, Kowa, Nagoya, Japan) and the fundus with a lens (MINI3000, Heine, Herrsching, Germany) after pupil dilation with 1% tropicamide (MSD-Chibret, Paris, France). Rabbits were euthanized with a lethal injection of intracardiac barbiturate (Dolethal, Vetoquinol, Lure, France) at different times after treatment: 2 h and 5, 21, 30 and 180 d.

Histologic analyses

Light microscopy. After fixation in a formol solution (at least 48 h), the eyes were dehydrated in alcohol solutions of increasing concentration, cleared in methylcyclohexane and embedded in paraffin (Automate ASP 300, Leica Microsystems, Wetzlar, Germany). They were sectioned coronally in two parts (one rostral, one caudal). The rostral portion was further sectioned in the coronal plane encompassing the ciliary processes. At least 30

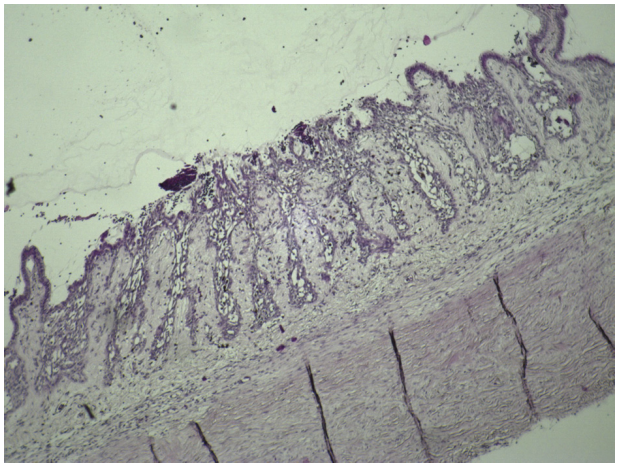

Fig. 2. Micrograph of an entire lesion at week 3, with coagulation necrosis, loss of the bilayered epithelium and distension of the stromal collagen fibers (×40).

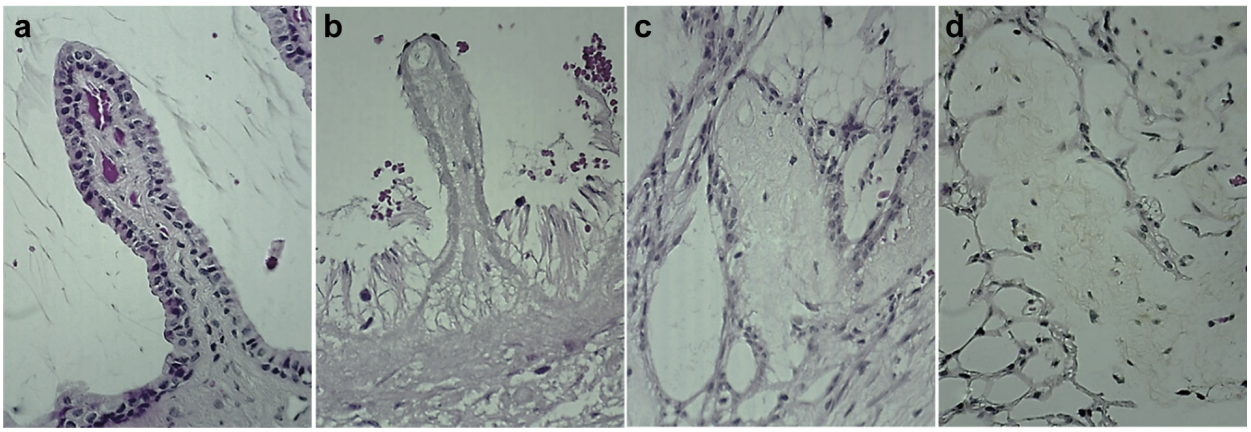

Fig. 3. High magnification (400×) micrographs of histologic slices revealing details of untreated ciliary processes (a) and ciliary process coagulation necrosis 5 d (b), 21 d (c) and 6 mo (d) after sonication.

serial sections (10 μm thick, every 100 μm) through the ciliary bodies were cut on a microtome (RM 2245, Leica Microsystems) and then stained with hematoxylin and eosin. Additional sections were performed when necessary to cut throughout the ciliary body. More anteriorly, radial sections of the trabecular meshwork were performed using the same microtome (10 μm thick, every 100 μm). The caudal portion of the eyes was further cut in a parasagittal plane to delimit a slice encompassing the optic nerve. Then, 15 sections (10 μm thick, every 300 μm) were performed and stained with hematoxylin and eosin at the level of the optic papilla. The sections were analyzed by light microscopy (Optika B-500Ti microscope fitted with 4×, 10× and 40× objectives and 10× eyepiece, Optika SRL, Bergamo, Italy).

Scanning electron microscopy. Eyes were sectioned coronally in two parts (one rostral, one caudal). The rostral portion was further sectioned in the coronal plane just behind the ciliary processes. The lens was detached during sectioning and then removed. The tissues were fixed in 4% glutaraldehyde and 0.2 M cacodylate buffer mixture 1:1 (pH 7.40), then washed in 0.4 M saccharose and 0.2 M cacodylate buffer (pH 7.40) 1:1. After several buffer solution rinses, the tissues were post-fixed in 2% osmium tetroxide and 0.3 M cacodylate buffer 1:1 and dehydrated in alcohol with graded concentrations before desiccation in hexamethyldisilazane. Samples were then introduced into the chamber of a sputter coater and coated with a very thin film (15 nm) of gold–palladium before examination by scanning electron microscopy (SEM) (S800 FEG, Hitachi, Tokyo, Japan).

Transmission electron microscopy. Eyes were sectioned coronally in two parts (one rostral, one caudal). The rostral portion was further sectioned in the coronal plane just behind the ciliary processes. The lens was detached during sectioning and then removed. The tissues were fixed in 4% glutaraldehyde and 0.2 M cacodylate buffer 1:1 (pH 7.40), then washed in 0.4 M saccharose and 0.2 M cacodylate buffer (pH 7.40) 1:1. After several buffer solution rinses, the tissues were post-fixed in 2% osmium tetroxide and 0.3 M cacodylate buffer 1:1 and dehydrated in alcohol with graded concentrations before being embedded in an epoxy resin. Subsequent ultrathin sections (70 nm) were obtained using an ultramicrotome (UC7, Leica, Solms, Germany) and then stained with uranyl acetate and lead citrate solutions and examined with a transmission electron microscope (CM120, Philips Electronics, Mahwah, NJ, USA).

Methacrylate resin corrosion casts. For these investigations, animals were anesthetized using the same procedures described earlier and then killed by bleeding to allow complete exsanguination. Each animal was prepared for casting by first isolating the jugular veins for

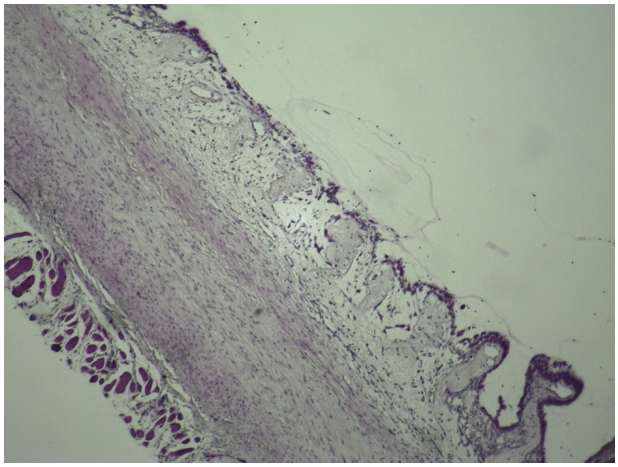

Fig. 4. Micrograph revealing the long-term aspects of treated ciliary processes and the ciliary body 1 m after sectorial sonication (×40). Appearance remained unchanged the following month.

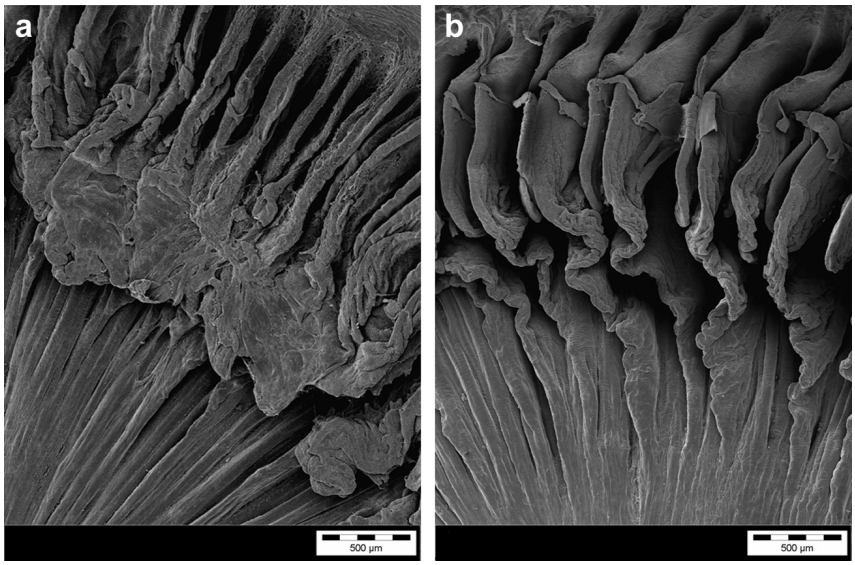

Fig. 5. (a) Micrograph of one spatially limited lesion including 12 adjacent ciliary processes, 6 mo after sonication. (b) Micrograph of control.

later transection. A catheter was then introduced into the carotid trough a midline incision, and the tip advanced to the level of the heart. Physiologic saline solution was perfused via the catheter with a syringe until the saline solution emerging from the jugular veins was completely clear of blood. A plastic mixture consisting of 10 mL of methyl methacrylate monomer solution catalyzed with 40% benzoyl peroxide in dibutyl phthalate (Mercox II Resin, Ladd Research, Williston, VT, USA) was manually injected and continued until resin flowed from the severed jugular veins. The injection pressure was 90 to 120 mm Hg. Tissues were allowed to rest for 30 min, and the eyes were enucleated and fixed in 10% formaldehyde overnight. Tissues were digested in 33% KOH at 45°C for 90 min. Castings were gently washed with running tap water and digested a second time to remove residual tissue. The castings were allowed to air-dry, and then anterior regions of the eyes were dissected free and mounted on metal SEM stubs and sputter-coated with gold–palladium for SEM (S800 FEG, Hitachi).

RESULTS

Intra-ocular pressure reduction and ophthalmic examinations

No complications occurred during any of the procedures. No significant abnormalities were observed during treatment. No macroscopic abnormalities of the eyes were observed after treatment. On post-treatment day 5, no abnormalities were observed during anterior segment and fundus examination. No phthisis occurred during the follow-up.

Values of IOP before and after treatment in the treated and control eyes are listed in Table 1. In treated eyes, IOP was significantly reduced after treatment, at each follow-up time point ($p < 0.0001$), whereas IOP

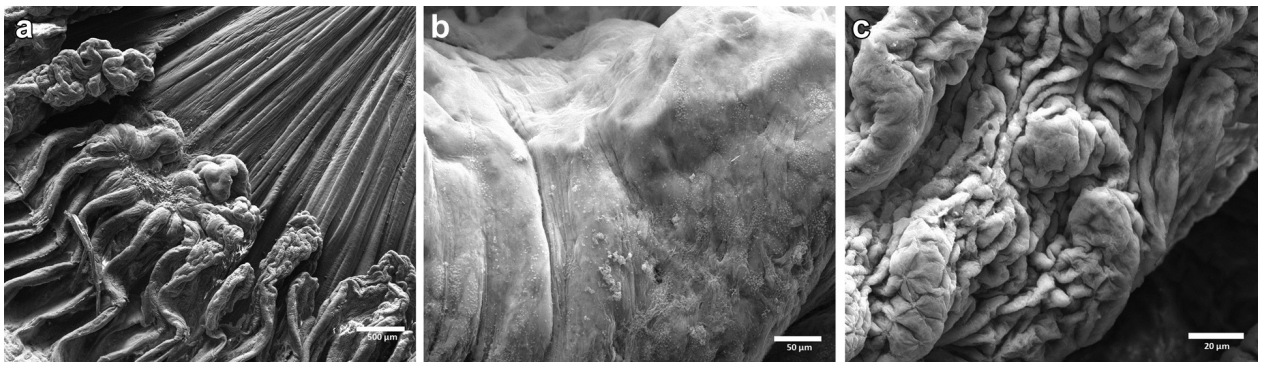

Fig. 6. Treated (a left, 60×; b, 1000×) and untreated (a right, 60×; c, 1000×) ciliary processes 5 d after sonication.

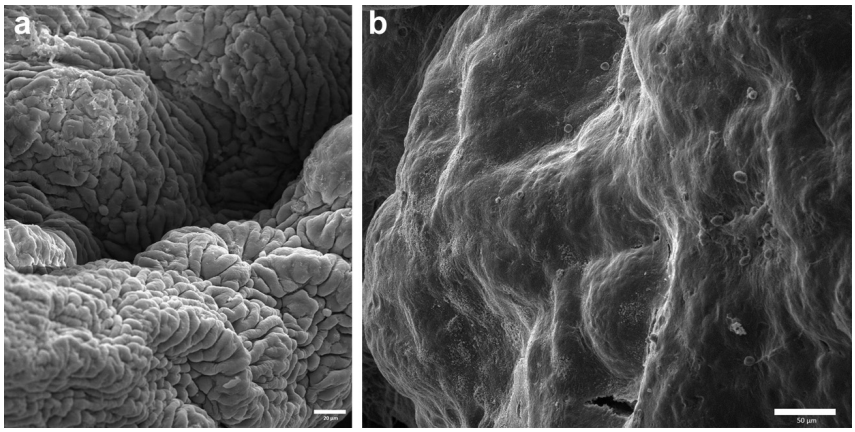

Fig. 7. Micrographs reveal differences between the surfaces of untreated (a, ×400) and treated (b, ×500) ciliary processes 5 d after sonication.

was not significantly reduced in control eyes during follow-up compared with baseline ($p > 0.5$).

Aqueous humor secretion structures

Light microscopy. From day 5 to week 3, histologic examinations performed in treated eyes revealed six circumferentially distributed areas of coagulation necrosis of the ciliary processes and ciliary body (Figs. 2 and 3). The six zones corresponded to the location of six transducers and were about 3 ± 0.5 mm wide (8–12 adjacent ciliary processes). The maximum intensity of coagulation necrosis was observed in the deepest regions of the ciliary processes, whereas the rostral and caudal regions were less affected. In the affected regions, the ciliary processes exhibited acute inflammatory and necrotic changes ranging from stromal edema (marked distension of collagen fibers) and vascular congestion (distension of vascular lumens by erythrocytes) to coagulation necrosis with loss of surface epithelium and hemorrhage. The bilayered epithelium was degenerated or necrotic and sloughed off in the intermediate and distal parts of the most affected areas. The ciliary stroma was free of fibroblasts and endothelial cells (Fig. 2). The inflammatory cellular reaction was very limited, with very small numbers of macrophages, lymphocytes, plasma cells, polymorphonuclear cells and giant cells. When examining the trabecular meshwork of the treated eyes, we never found any deposits of residues coming from the ciliary epithelium in the structures of the trabecular meshwork and never found any macrophage cells and/or other inflammatory cells or histologic changes of the trabecular lamellae.

From month 1 to month 6, histologic examinations revealed involution of the ciliary processes, with short

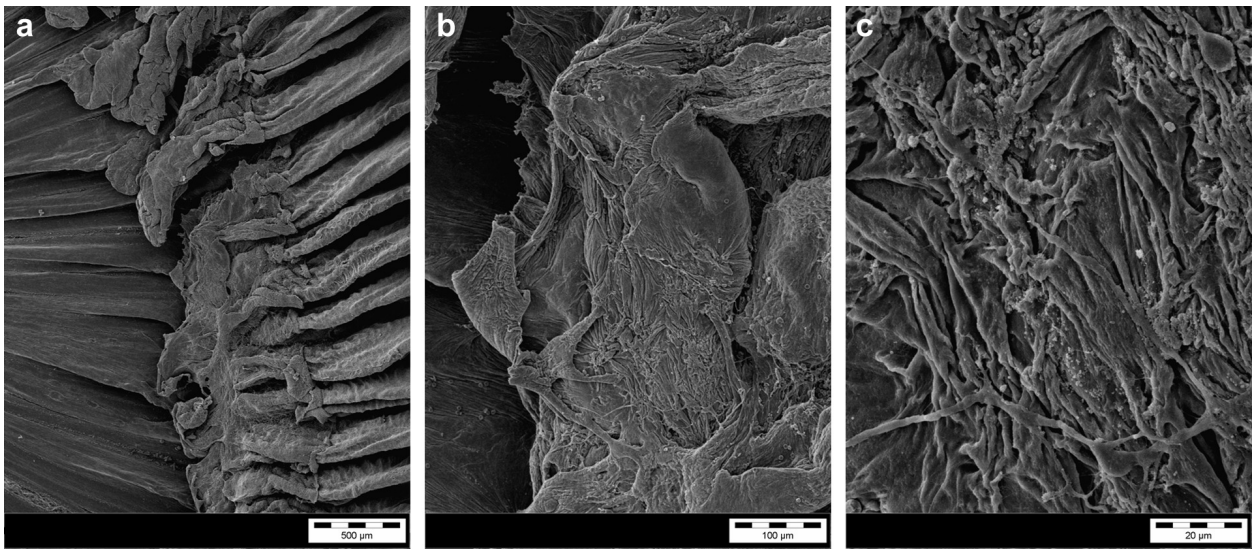

Fig. 8. Micrographs of the surfaces of treated ciliary processes (a–c, increasing magnification) 6 mo after sonication.

or absent ciliary processes covered by a non-bilayered epithelium and composed of dimorphic and likely non-functional cells (Figs. 3 and 4). The deeper layer was usually absent. The width of the affected area appeared unchanged compared with those of the lesions observed from day 5 to month 1, and were about 3 ± 0.5 mm wide (8–12 adjacent ciliary processes, see Fig. 4). Because of the involution of the ciliary processes, the total surface of the neo-formed epithelium was notably reduced compared with that of controls. We consistently observed late scleral thinning adjacent to the treated areas (see Figs. 4 and 12D, 12E). The width of the sclera thinning areas was similar or slightly lower than the ciliary coagulation necrosis area width (2.7 ± 0.8 mm). The thickness of the sclera in the thinnest point was about 62 ± 14% of the thickness of the unaffected sclera.

Scanning electron microscopy. Scanning electron microscopy of treated eyes revealed lesions spatially limited to 8–12 adjacent ciliary processes (Fig. 5) for each area of single ultrasound exposure. In the first week after sonication, ciliary processes appeared bulky, probably

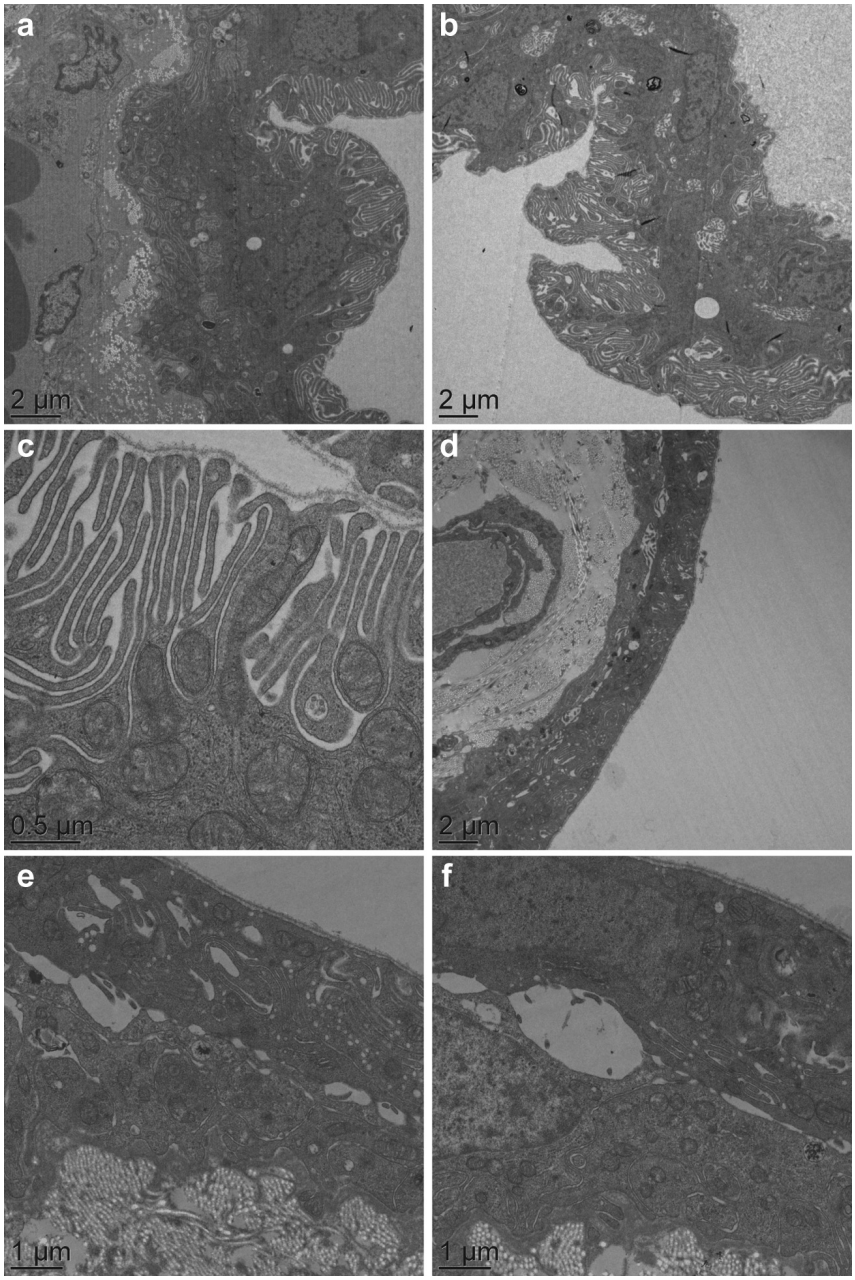

Fig. 9. Micrographs reveal the differences between epithelia of untreated (a–c) and treated (d–f) ciliary processes 6 mo after sonication. Note the cleavage between the two layers of the neo-formed epithelium (d–f).

because of stromal edema. Higher-magnification images showed a smooth membrane likely corresponding to the basal membrane without any residual epithelial cells (Figs. 6 and 7). One month after treatment and later, scanning electron microscopy revealed involution and atrophy of the treated ciliary processes (Figs. 5 and 8). The surface of the latter was partially covered by a disorganized epithelium composed of dysmorphic and flattened cells. By contrast, images of the adjacent untreated areas revealed a normal ciliary epithelium, with ciliary processes covered by numerous epithelial cells (Fig. 7). Fibrin deposits were usually very limited or absent.

Transmission electron microscopy. Transmission electron microscopy of the treated ciliary epithelium performed from month 1 to month 6 after treatment revealed a dimorphic mono- and/or bilayered epithelium. Epithelial cells appeared thinner and had much fewer apical villi than the cells of the untreated epithelium (Fig. 9). When the neo-formed epithelium was bilayered, areas of cleavage were frequently seen between the two layers of cells. The cytoplasm of the non-pigmented cells had few or no mitochondria, whereas the non-pigmented cells in the untreated areas or in the control eyes had several mitochondria. The cytoplasm of the pigmented layer had no or few pigment granules. The basal membrane of the epithelial cells was disrupted. Transmission electron microscopy of the treated ciliary stroma performed from month 1 to month 6 after treatment revealed some fibroblasts surrounded by the extracellular matrix. Few vessels and endothelial cells surrounding the vessels were observed.

Methacrylate resin corrosion casts. Light microscopy and scanning electron microscopy of vascular corrosion casts performed after intravascular injection of methacrylate resin revealed focal interruption of the ciliary body and pars plana microvasculature (Figs. 10, 11). At the end of the disrupted vessels, the resin had left the vessel lumen and formed drop-like extravasations. This aspect was found both the first weeks after treatment and later, without neovascularization at the margins of the defect areas. Vascular defects were limited to the treatment areas and had dimensions comparable to those of lesions observed with light or scanning electron microscopy (3 ± 0.5 mm wide and 1.2 ± 0.7 mm anterior–posterior length). The 3-D architecture of the microvasculature of the untreated areas of the ciliary body and ciliary processes appeared intact. The major and minor arterial iris circles appeared undamaged. The vascular network of the iris and iris root was not damaged.

Aqueous outflow pathways

Light microscopy. In treated eyes, histologic examinations performed from day 5 to 1 month revealed several large fluid spaces between the sclera and the ciliary body, between the sclera and the choroid and inside the basal part of the ciliary body. These fluid spaces were observed next to treated areas, but not next to untreated areas or in control eyes (Fig. 12). This characteristic was maintained up to month 6 (see Figs. 12E, 12F), likely indicating that it is due to tissue retraction or tissue micro-architecture changes rather than intra-ocular inflammation. The width of the areas having fluid spaces was similar or slightly greater than the ciliary body coagulation necrosis area width (3.4 ± 1.1 mm). Residual tissue bridges were frequently found inside the fluid spaces. As mentioned

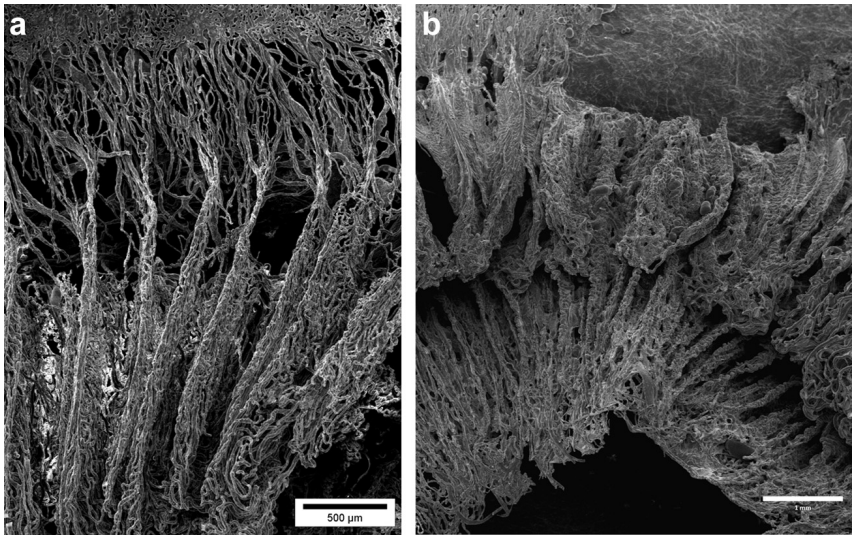

Fig. 10. Low-magnification scanning electron microscopy images of vascular corrosion cast performed after intravascular injection of methacrylate resin and after tissue dissolution in an untreated eye (a) and a treated eye (b), revealing a focal defect of the ciliary body microvasculature.

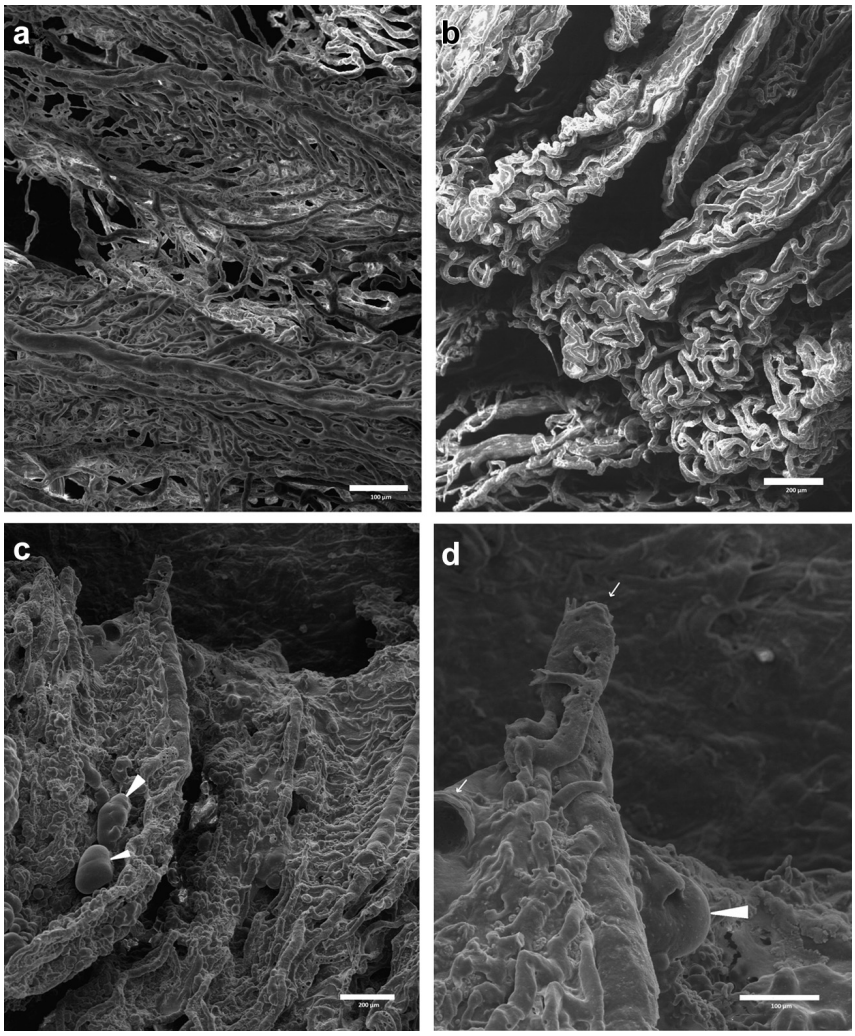

Fig. 11. Scanning electron microscopy images of vascular corrosion cast in untreated (a, b) and treated (c, d) eyes, revealing a marked defect in the capillary network of the ciliary body (*white arrows*), with mixture extravasation at the end of the disrupted vessels (*white arrowheads*).

earlier, long-term scleral thinning was also observed in almost all treated eyes, near the sectors treated (see Fig. 12E).

DISCUSSION AND CONCLUSIONS

We conducted the present study to investigate the multiple possible short- and long-term effects of high-intensity focused ultrasound cyclocoagulation on both the aqueous humor production structures and aqueous outflow pathways in rabbits. We observed marked and sustained focal coagulation necrosis of the ciliary processes, sustained focal interruption of the ciliary body and pars plana vascularization, the presence of a diffuse and sustained fluid space between the sclera and the choroid and late scleral thinning adjacent to the areas of treatment.

With respect to aqueous production, a few weeks/months after sonication, we observed selective coagulation necrosis of the treated ciliary processes, without damage to the untreated areas. We could hypothesize that those damages in the bilayered epithelium result in reduced aqueous production. However, it should be mentioned that processes located among areas of treatment remained intact. Light microscopy and scanning electron microscopy revealed that each area of treatment included 8 to 12 adjacent ciliary processes, resulting in coagulation of about 50 to 70 ciliary processes when the six transducers of the device were activated. New Zealand White rabbits usually have 100 to 120 major ciliary processes. It is likely that the remaining ciliary processes allow significant aqueous residual secretion. Months after treatment, we observed moderate epithelial regeneration covering shortened and flattened ciliary processes. However, the mono- or bilayered epithelium was always disorganized and composed of thin cells devoid of apical villi and with frequent detachment of the two

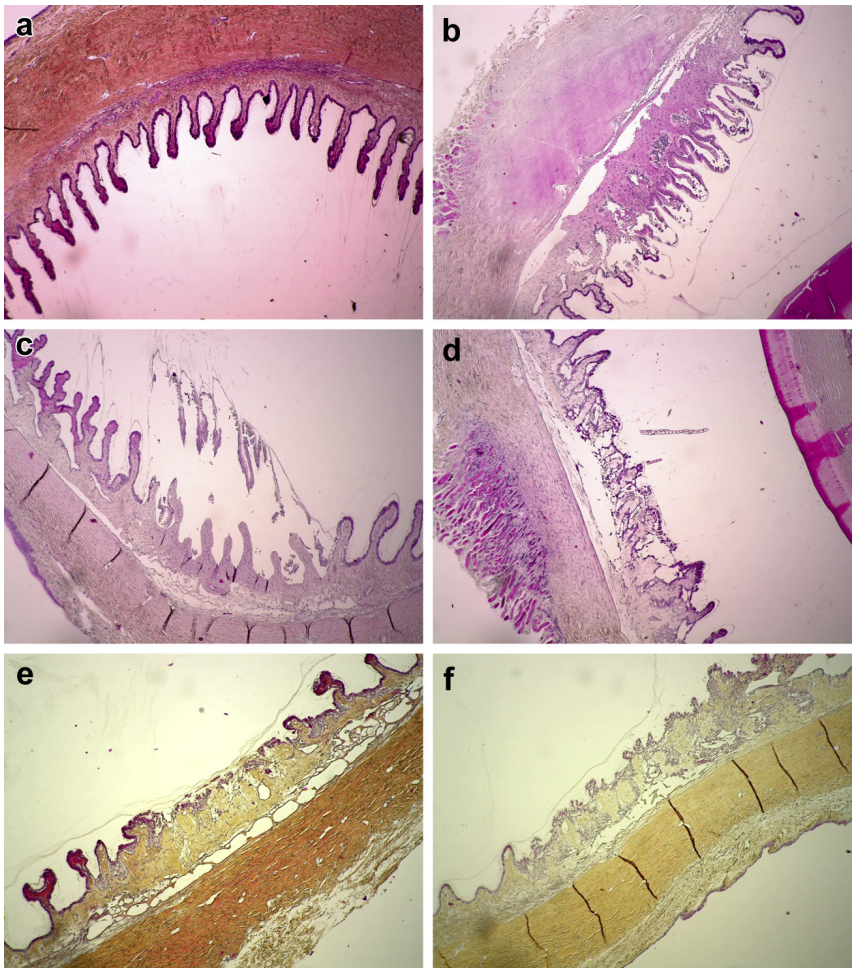

Fig. 12. Photomicrographs (×40) revealing a fluid space between the sclera and the ciliary body adjacent to a treated sector demonstrating ciliary process coagulation necrosis and loss of ciliary epithelium, 2 h (b), 5 d (c), 21 d (d) and 6 mo (e, f) after sonication. (a) Control.

layers. We could therefore presume that this epithelium is non-functional from a secretory point a view. Moreover, as the ciliary processes are notably shortened, the total surface of the unfolded neo-formed ciliary epithelium is reduced. Previous studies performed after diode or Nd:YAG laser cyclophotocoagulation revealed similar findings, in both rabbits and humans (Blasini et al. 1990; Brancato et al. 1991; Ferry et al. 1995; Liu et al. 1994; McKelvie and Walland 2002; Pantcheva et al. 2007; Schlote et al. 2001).

By using vascular corrosion casts, we observed complete focal destruction of the vascular network of the ciliary body and pars plana. This aspect was conserved several months after treatment. This long-term depletion of the vascular supply of the treated areas likely partially explains the atrophy of the ciliary processes observed months after treatment—shortening and flattening of the ciliary processes—and the dimorphic aspect of the neo-formed epithelium. This sustained destruction of the capillary network of the ciliary body and processes also reinforces the supposition that the neo-formed epithelium is non-functional from a secretory point a view, as the hydrostatic pressure in the stroma of the ciliary processes devoid of blood capillaries should be strongly reduced. Adjacent to the treated areas, the 3-D architecture of the microvasculature of the ciliary body and ciliary processes appeared intact, also reinforcing the hypothesis that the untreated parts of the ciliary body should remain functional and secreting. More anteriorly, the major and minor arterial iris circles appeared undamaged. This integrity of the blood–aqueous barrier corroborates the lack of histologic signs of early or late ocular inflammation. Regarding the vascular effects of cyclophotocoagulation, our results are very similar to those reported after diode laser and Nd:YAG transscleral cyclophotocoagulation in rabbits (Schlote et al. 2001; Van der Zypen et al. 1989; Lin et al. 2006). Regarding aqueous outflow, light microscopy revealed a fluid space between the sclera and the ciliary body and between the sclera and the choroid adjacent to treated

areas. This characteristic seems to be maintained over time, likely indicating that it is due to tissue retraction or tissue micro-architecture changes rather than intraocular inflammation, and was not observed in untreated eyes, thus eliminating the possibility of an artifact of tissue preparation. Previous studies using light microscopy or tracer particles have also reported or supposed an increase of the aqueous outflow after various methods of cyclocoagulation (Liu et al. 1994; Polack et al. 1991; Coleman et al. 1985). An increase in the outflow by the uveoscleral pathway and the formation of a new outflow tract from the posterior chamber through a necrotic or thinned ciliary body and pars plana have been advanced to explain the outflow increase.

In summary, we found that ultrasonic coagulation of the ciliary body using high-intensity focused ultrasound could result in a dual effect on the dynamics of aqueous humor contributing to reduction of IOP. We do not know the respective parts of the aqueous secretion decrease and aqueous outflow increase. Some evidence, such as the spatially limited area of ciliary epithelium coagulation, could dispute the aqueous secretion decrease as the primary mechanism of IOP reduction. A more definitive answer would require *in vivo* fluorophotometric and tonographic quantification of the aqueous inflow and outflow. From a clinical point of view, those findings could indicate that it could be pertinent to target the basal part of the ciliary body and the junction of the ciliary body and sclera when choosing the diameter and orientation of the probe from ultrasound biomicroscopy images before treatment (Aptel et al. 2011). A possible dominant effect of the aqueous outflow increase and the conservation of a significant aqueous humor secretion could also explain the rather good tolerability of the method in humans, particularly the lack of ocular phthisis bulbi, even after repeated treatments (Aptel et al. 2011; Rouland and Aptel 2013).

Acknowledgments—The authors thank David Clément (EyeTechCare, employee) for technical support, the Centre Commun d'Imagerie de Lyon-Est (Lab CeCILE, Lyon, France) and the Centre Technologique des Microstructures de l'UCBL Lyon1 (CTM, Lyon, France) for their contribution to scanning and transmission microscopy studies, and the Centre d'Histopathologie du Petit Animal de laboratoire (Lab Anipath, Lyon, France) for their contribution to light microscopy studies. This work was partially supported by EyeTechCare (Rillieux la Pape, France).

REFERENCES

Al-Ghamdi S, Al-Obeidan S, Tomey KF, Al-Jadaan I. Transscleral neodymium:YAG laser cyclophotocoagulation for end-stage glaucoma, refractory glaucoma, and painful blind eyes. Ophthalmic Surg 1993; 24:526–529.

Aptel F, Charrel T, Lafon C, Romano F, Chapelon JY, Blumen-Ohana E, Nordmann JP, Denis P. Miniaturized high-intensity focused ultrasound device in patients with glaucoma: A clinical pilot study. Invest Ophthalmol Vis Sci 2011;52:8747–8753.

Aptel F, Charrel T, Palazzi X, Chapelon JY, Denis P, Lafon C. Histologic effects of a new device for high-intensity focused ultrasound cyclocoagulation. Invest Ophthalmol Vis Sci 2010;51:5092–5098.

Aptel F, Lafon C. Therapeutic applications of ultrasound in ophthalmology. Int J Hyperthermia 2012;28:405–418.

Blasini M, Simmons R, Shields MB. Early tissue response to transscleral neodymium:YAG cyclophotocoagulation. Invest Ophthalmol Vis Sci 1990;31:1114–1118.

Brancato R, Leoni G, Trabucchi G, Cappellini A. Histopathology of continuous wave neodymium:yttrium aluminum garnet and diode laser contact transscleral lesions in rabbit ciliary body: A comparative study. Invest Ophthalmol Vis Sci 1991;32:1586–1592.

Charrel T, Aptel F, Birer A, Chavrier F, Romano F. Development of a miniaturized HIFU device for glaucoma treatment with conformal coagulation of the ciliary bodies. Ultrasound Med Biol 2011;37: 742–754.

Coleman DJ, Lizzi FL, Driller J, Rosado AL, Chang S, Iwamoto T, Rosenthal D. Therapeutic ultrasound in the treatment of glaucoma: I. Experimental model. Ophthalmology 1985;92:339–346.

De Roetth A Jr. Cryosurgery for the treatment of glaucoma. Trans Am Ophthalmol Soc 1965;63:189–204.

Ferry AP, King MH, Richards DW. Histopathologic observations on human eyes following neodymium:YAG laser cyclophotocoagulation for glaucoma. Trans Am Ophthalmol Soc 1995;93:315–331.

Hamard P, Gayraud JM, Kopel J, Valtot F, Quesnot S, Hamard H. Treatment of refractory glaucomas by transscleral cyclophotocoagulation using semiconductor diode laser: Analysis of 50 patients followed up over 19 months. J Fr Ophthalmol 1997;20:125–133.

Kosoko O, Gaasterland DE, Pollack IP, Enger CL. Long-term outcome of initial ciliary ablation with contact diode laser transscleral cyclophotocoagulation for severe glaucoma: The Diode Laser Ciliary Ablation Study Group. Ophthalmology 1996;103:1294–1302.

Lin SC, Chen MJ, Lin MS, Howes E, Stamper RL. Vascular effects on ciliary tissue from endoscopic versus trans-scleral cyclophotocoagulation. Br J Ophthalmol 2006;90:496–500.

Liu GJ, Mizukawa A, Okisaka S. Mechanism of intraocular pressure decrease after contact transscleral continuous-wave Nd:YAG laser cyclophotocoagulation. Ophthalmic Res 1994;26:65–79.

Maus M, Katz LJ. Choroidal detachment, flat anterior chamber, and hypotony as complications of neodymium: YAG laser cyclophotocoagulation. Ophthalmology 1990;97:69–72.

McKelvie PA, Walland MJ. Pathology of cyclodiode laser: A series of nine enucleated eyes. Br J Ophthalmol 2002;86:381–386.

Pantcheva MB, Kahook MY, Schuman JS, Rubin MW, Noecker RJ. Comparison of acute structural and histopathological changes of the porcine ciliary processes after endoscopic cyclophotocoagulation and transscleral cyclophotocoagulation. Clin Experiment Ophthalmol 2007;35:270–274.

Polack PJ, Iwamoto T, Silverman RH, Driller J, Lizzi FL, Coleman DJ. Histologic effects of contact ultrasound for the treatment of glaucoma. Invest Ophthalmol Vis Sci 1991;32:2136–2142.

Rouland JF, Aptel F. Treatment of glaucoma using UC procedure with high-intensity focused ultrasound (HIFU): Prospective series. Invest Ophthalmol Vis Sci 2013;54. E-Abstract 451.

Sabri K, Vernon SA. Scleral perforation following trans-scleral cyclodiode. Br J Ophthalmol 1999;83:502–503.

Schlote T, Beck J, Rohrbach JM, Funk RH. Alteration of the vascular supply in the rabbit ciliary body by transscleral diode laser cyclophotocoagulation. Graefes Arch Clin Exp Ophthalmol 2001;239:53–58.

Schubert HD, Federman JL. The role of inflammation in CW Nd:YAG contact transscleral photocoagulation and cryopexy. Invest Ophthalmol Vis Sci 1989;30:543–549.

Uram M. Ophthalmic laser microendoscope ciliary process ablation in the management of neovascular glaucoma. Ophthalmology 1992; 99:1823–1828.

Van der Zypen E, England C, Fankhauser F, Kwasniewska S. The effect of transscleral laser cyclophotocoagulation on rabbit ciliary body vascularization. Graefes Arch Clin Exp Ophthalmol 1989;227:172–179.

Vernon SA, Koppens JM, Menon GJ, Negi AK. Diode laser cycloablation in adult glaucoma: Long-term results of a standard protocol and review of current literature. Clin Experiment Ophthalmol 2006;34: 411–420.